AMERICAN SOCIETY FOR MICROBIOLOGY | Antimicrobial Agents and Chemotherapy

Check for updates

A propidium iodide-based *in vitro* screen of the "Bug Box" against *Babesia duncani* reveals potent inhibitors

Emmett A. Dews,[1,2] José E. Teixeira,[1] Christopher D. Huston,[1,2,3] Marvin J. Meyers,[4] Peter R. Hyson[1]

AUTHOR AFFILIATIONS See affiliation list on p. 12.

ABSTRACT The incidence and endemic range of human babesiosis are expanding. Standard therapy for human babesiosis consists of antimicrobials developed for other indications. While these treatments are adequate in immunocompetent hosts, infections in the immunocompromised can be severe, relapsing, and drug-resistant despite the use of multi-drug regimens. Existing drugs are ineffective in the immunocompromised because they cannot achieve and maintain adequate serum concentrations to inhibit *Babesia*. Discovery of improved agents against *Babesia* spp. is of growing importance, and efficient techniques for high-throughput compound screening can assist in this effort. We developed a high-throughput *in vitro* drug screening assay for *Babesia duncani* that is conducted in 384-well plates and makes use of the fluorescent DNA stain propidium iodide (PI) with relative fluorescence measured by a microplate reader. A Z′ factor of 0.82 was calculated, which suggests an excellent ability to detect inhibitory compounds. A screen of the 41-compound library Structural Genomics Consortium Bug Box was conducted, yielding five hits: trimethoprim, atovaquone, SDDC M7, diphenyleneiodonium chloride, and panobinostat. Panobinostat, a histone deacetylase complex (HDAC) inhibitor, was selected for further evaluation given that its target had not been previously explored in *B. duncani*. Dose-response testing of structurally related compounds revealed multiple potential leads, including nanatinostat and quisinostat, both of which were potent at the nanomolar level and showed favorable selectivity index in cytotoxicity studies. High-throughput screening using PI and 384-well plates is an advance in drug discovery for babesiosis, and HDAC inhibitors show promise as lead compounds worthy of further investigation.

KEYWORDS babesiosis, *Babesia duncani*, drug discovery, histone deacetylase inhibitors, drug screening assay

Babesiosis, the disease caused by the intracellular parasite *Babesia*, is an emerging infectious disease with rising incidence and expanding endemic range (1–3). *Babesia* are tickborne, malaria-like protozoa of the phylum Apicomplexa which infect red blood cells of vertebrates, including humans. The spectrum of human disease is wide, with many infections asymptomatic or causing a mild, self-limited, flulike illness, but a few—particularly in patients at the extremes of age or with compromised immune systems—leading to critical illness and even death (4). Patients with asplenia are at particularly high risk of fulminant disease due to their inability to clear the bloodstream of infected erythrocytes.

Standard of care antimicrobial treatment for Babesiosis consists of combination therapy using clindamycin/quinine or atovaquone/azithromycin, antimicrobials developed and dosed for other indications such as malaria (5). While this treatment is generally effective in immunocompetent patients, in immunocompromised hosts, infections can be relapsing and even incurable despite the use of multi-drug regimens, and antimicrobial resistance can develop during therapy (6–8). Indeed, evidence from

Editor Audrey Odom John, The Children's Hospital of Philadelphia, Philadelphia, Pennsylvania, USA

Address correspondence to Peter R. Hyson, peter.hyson@med.uvm.edu.

The authors declare no conflict of interest.

Received 10 January 2025
Accepted 16 April 2025
Published 9 June 2025

Copyright © 2025 Dews et al. This is an open-access article distributed under the terms of the Creative Commons Attribution 4.0 International license.

animal models and *in vitro* culture suggests that most of the standard antimicrobial agents used for this indication have poor efficacy with minimum inhibitory concentrations (MICs) orders of magnitude higher in *Babesia* than *Plasmodium*, treatment failure in SCID mice, and rapid development of antimicrobial resistance on single-agent therapy (9–12). Identification of new therapies against *Babesia* is of increasing concern given the expansion of this disease and the large and growing population of persons with asplenia and other immunocompromising conditions (13).

High-throughput screening can be an efficient way to identify compounds that have activity for a particular indication and new drug targets that can be leveraged with rational drug design. Such an assay needs to be rapid, reproducible, capable of testing large numbers of compounds in small quantities, and capable of accurately distinguishing hits from compounds that lack significant activity. An *in vitro* drug screening assay using miniaturized cultures of *Babesia* in 96-well plates and SYBR green fluorescent labeling to identify infected erythrocytes has been developed and validated with *B. bovis* and utilized widely for multiple *Babesia* species (9, 14–16). To our knowledge, however, validation of such an assay in 384-well plates and using the inexpensive reagent propidium iodide (PI) has not been described. The use of the 384-well plate for high-throughput screening is beneficial because it increases the number of compounds that can be simultaneously screened, uses less compound, and is more cost-effective. *Babesia duncani* is an ideal organism to use for drug discovery using high-throughput screening, as it may both be continuously cultured *in vitro* (unlike the prevalent human pathogen *B. microti*) and because it has a murine model that may be used for further characterization and optimization of lead compounds (17). Herein, we describe the optimization of a high-throughput, PI-based drug screening assay for *B. duncani* and the deployment of this assay in screening a collection of 41 compounds with reported antimicrobial activity that was previously assembled by the Structural Genomics Consortium (18). We report the identification and characterization of novel classes of potent anti-*Babesia* compounds.

RESULTS

Propidium-iodide-based drug assay optimization

Diluting parasitemia experiments were performed iteratively to optimize the PI staining protocol. Figure 1A illustrates a close correlation between fluorescence from PI staining and parasitemia, as shown in two independent experiments with R^2 >0.95.

Growth kinetics experiments were also performed to assess the ability of *B. duncani* to propagate in miniaturized culture conditions. Figure 1B shows the 48 hours of growth of *B. duncani* in a 96-well plate with multiple different starting parasitemias. Figure 1C shows the 72 hours of growth of *B. duncani* in a 384-well plate as measured by PI staining and fluorescence, with results of manually scoring blood smears indicated in the text. It was established that in a culture of 5% hematocrit and with starting parasitemia of 7.5%, 48 hours of parasitemia could be expected to be >20% in a 384-well plate. In a 96-well plate, parasitemia would more than triple in the course of 48 hours, where starting parasitemia was 2.5%–10%. Moreover, parasite growth could be accurately and reproducibly measured with PI staining and microplate fluorimetry.

Assay validation for library screening

The Z or Z′-score, a statistical coefficient that describes an assay's signal window, is commonly used to assess an assay's suitability for compound library screening, with Z-scores of 0.5–1 indicating an excellent assay (19). PI is expected to stain persistent DNA from killed or inhibited *Babesia*. We therefore determined the Z′-score by comparing the fluorescence of untreated infected wells to infected wells treated with the dihydrofolate reductase inhibitor WR99210, a known inhibitor of *Babesia* growth (20). As shown in Fig. 1D, this experiment yielded a Z′ score of 0.82, consistent with an excellent ability to detect an effective inhibitory agent (19).

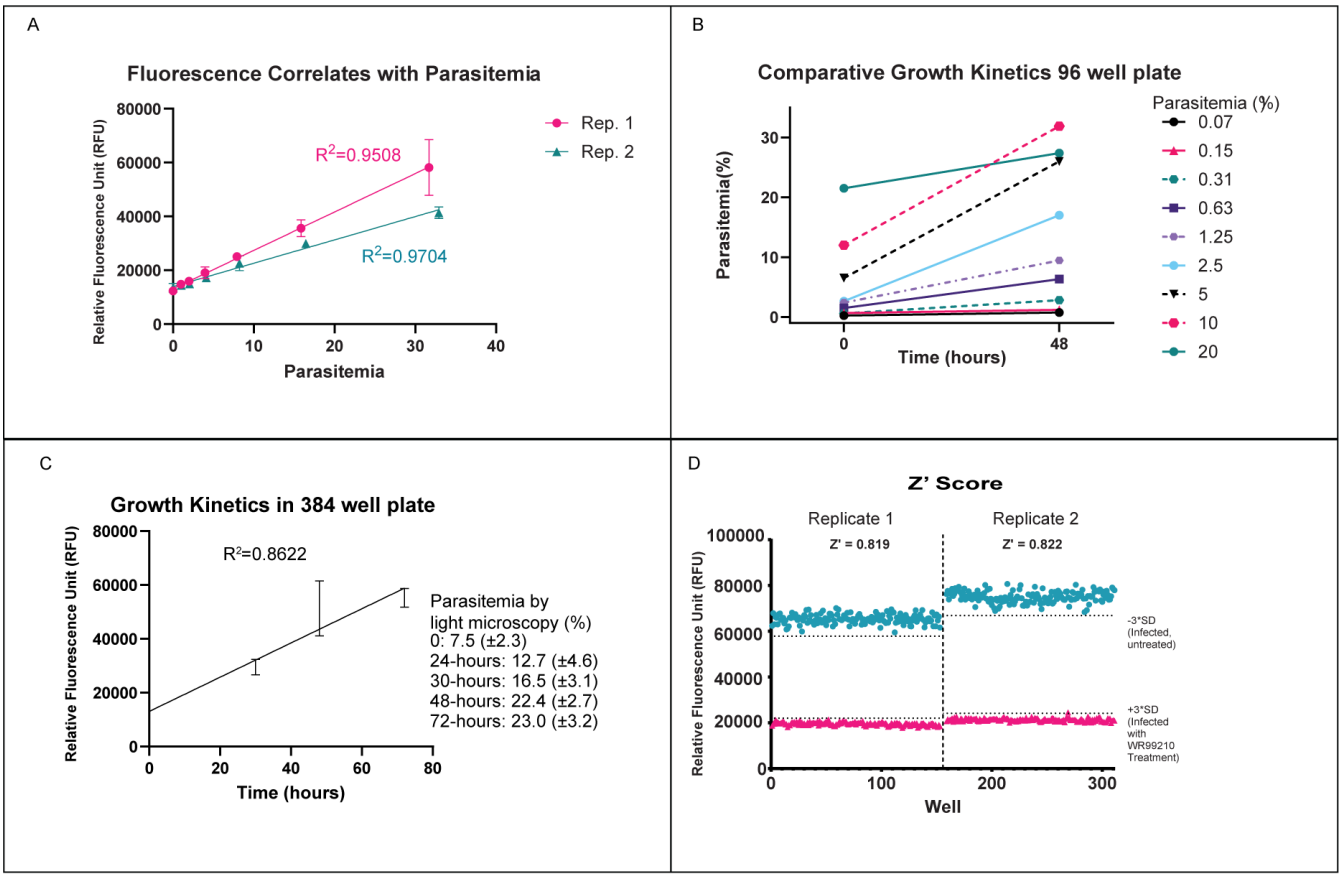


FIG 1 (A) Serial dilutions of high parasitemia *B. duncani* were made and seeded into a 384-well plate with three well technical replicates. Wells were stained with PI and then read using a microplate reader. Both repeats of this experiment are shown with a mean and standard deviation displayed. (B) *B. duncani*-infected red blood cells were seeded into a 96-well plate at different starting parasitemias and incubated for 48 hours. Parasites were manually counted from Giemsa-stained blood smears at time 0 and 48 hours. Each point represents parasitemia of a single well. (C) *B. duncani*-infected red blood cells were seeded into 384-well plates at a parasitemia of 7.5% and then analyzed at 24, 30, 48, and 72 hours, with parasitemia measured using both PI staining (mean and standard deviation on graph) and blood smears and manual parasite counting (average and standard deviation in legend). Time zero point included 22 wells, the 24-hour time point included 28 wells, and all others were 27-well technical replicates. (D) Half of a 384-well plate was seeded with *B. duncani*-infected red blood cells and treated for 48 hours with WR99210, while half was incubated with DMSO vehicle. The plate was then stained with PI and read with a microplate reader. Z′ score calculated as described in Materials and Methods. Both experiment replicates are displayed.

Pilot testing of the vehicle and known compounds

Having optimized staining protocols and culture conditions, dose-response assays were conducted with DMSO vehicle, WR99210 (control agent with known inhibitory activity on *B. duncani*), and standard of care drugs atovaquone, azithromycin, clindamycin, and quinine. Results are shown in Fig. 2. DMSO, the vehicle in which experimental compounds are dissolved, lacked significant inhibitory activity at concentrations up to 0.5% by volume. WR99210 was demonstrated to have a 50% effective concentration (EC50) of 8.3 nM while atovaquone was also quite potent with EC50 of 518 nM. Azithromycin and quinine were only modestly effective with EC50s of 12.37 and 17.49 µM, respectively. Clindamycin appeared not to inhibit at all.

Pilot screen & hit validation

The SGC previously assembled a small collection of known antimicrobial compounds (the "Bug Box") that we used to test our assay in practice while identifying new anti-*Babesia* compounds (18). Compounds were screened at 5 µM and 1 µM, and compounds that inhibited greater than 80% were selected for re-supply and dose-response testing.

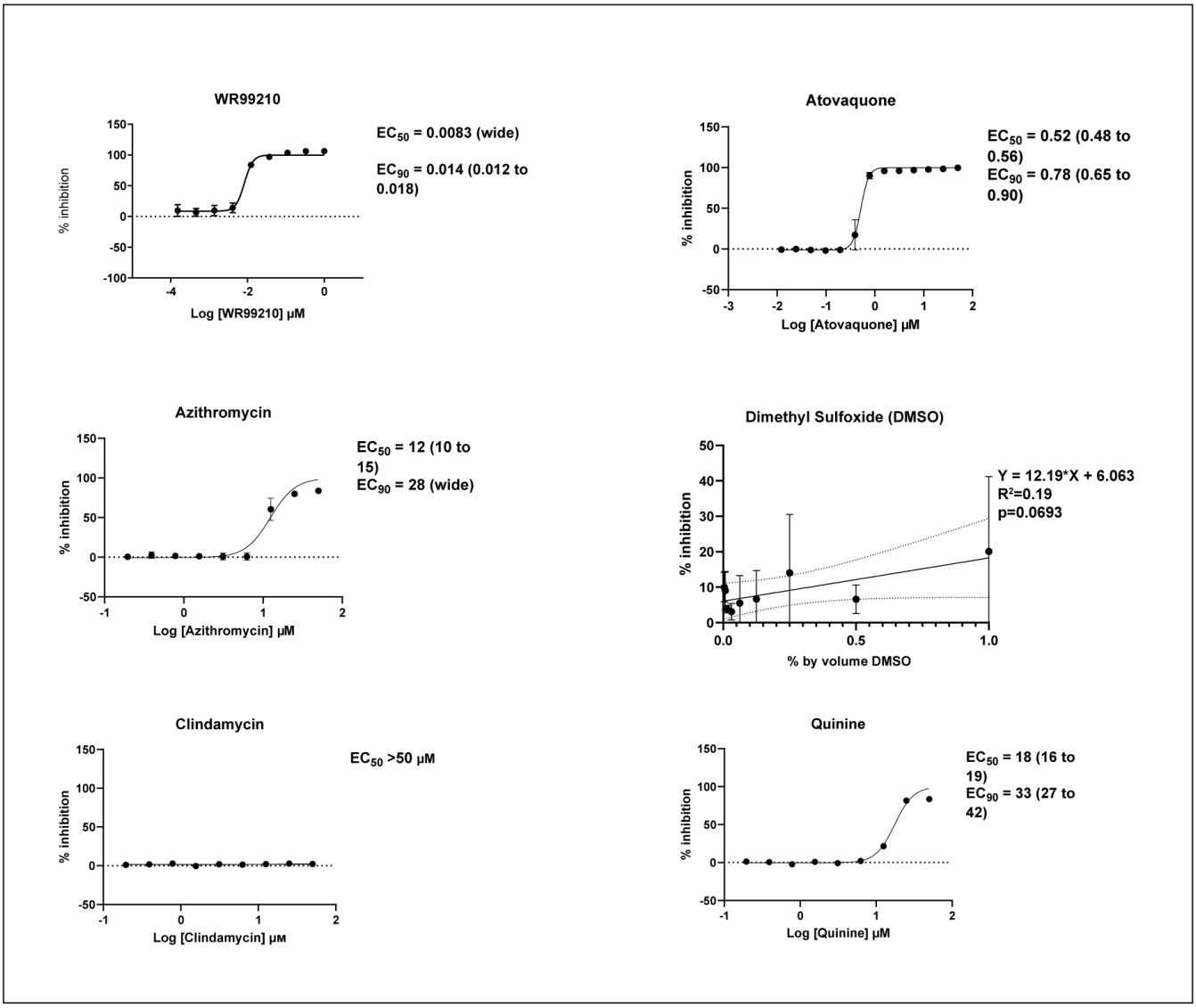


FIG 2 Dose-response curves for standard of care compounds and control compounds with *B. duncani in vitro*. Generated using a nine-point serial dilution of the compound and treatment of parasite-infected red blood cells in 384-well plates with 48 hours of incubation and propidium iodide staining. Four technical replicate wells per compound dilution and experiments repeated twice with EC50, EC90, and 95% CI for each reported. Mean and standard deviation are shown for each dilution. WR99210 is a DHFR inhibitor commonly used in experiments with *Babesia*. DMSO is used as a drug vehicle in our experiments. DMSO dilutions were calculated and measured in percent by volume, and analysis was performed with simple linear regression, with no correlation between dose and inhibition.

Five compounds met the hit definition at 5 µM: panobinostat, trimethoprim, diphenylene iodonium chloride, atovaquone, and SDDC M7 (Fig. 3A). Figure 3B shows the results of dose-response testing with commercially resupplied compounds. Atovaquone was not retested as it is known to be inhibitory toward *Babesia,* and an EC50 had been generated previously. While trimethoprim proved only modestly effective with an EC50 of 2.7 µM, the remaining three agents were very potent inhibitors of *Babesia duncani* growth *in vitro*. The histone deacetylase (HDAC) inhibitor panobinostat was most impressive with an EC50 of 8.4 nM, followed by SDDC M7 at 28 nM and diphenylene iodonium chloride at 550 nM.

Histone deacetylase complex inhibitor testing

In light of the high potency of panobinostat and the novelty of the putative target (HDAC) in *Babesia duncani,* we decided to test other structurally related and unrelated

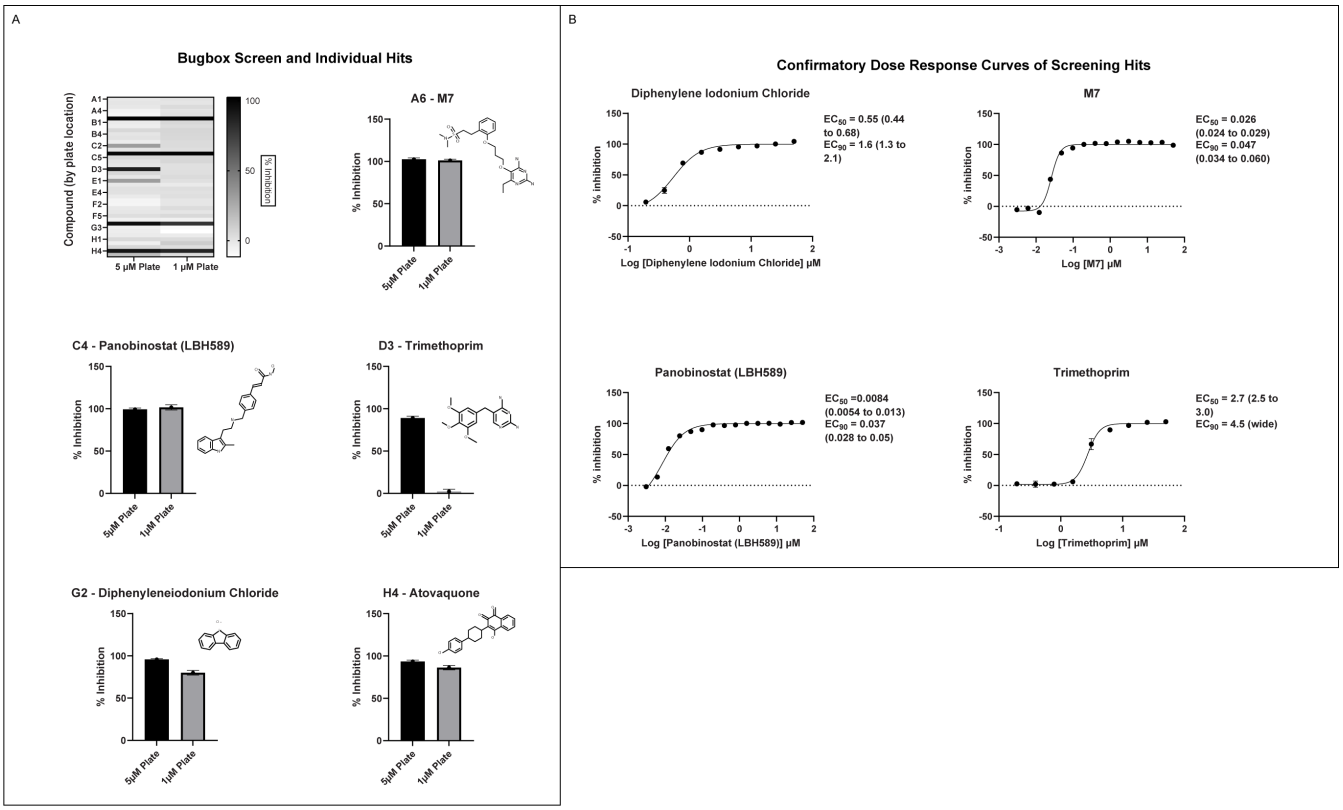


FIG 3 Bug Box initial screen and hit validation (A) Screen of the Bug Box was run in two 384-well plates, with one testing 1 µM dilutions and the other 5 µM compound dilutions with *B. duncani*-infected red blood cells. Heatmap shows relative inhibitory activity by compound location in the plate, with darker bars indicating greater inhibition and hits magnified. (B) Validation of hits with dose-response curves using compounds commercially obtained (with the exception of M7). Atovaquone was excluded as it had been previously validated. Each dose-response experiment was repeated twice, with a graph showing combined data. Mean and standard deviation are shown for each dilution. EC50s and EC90s are reported with 95% confidence intervals.

HDAC inhibitors. A selection of commercially available HDAC inhibitors was chosen from among hydroxamates and benzamides, which had been either approved for clinical use or had reached late stages of development (21). Dose-response curves were generated with EC50s given in Table 1. All of the compounds tested proved to have inhibitory activity, most with EC50s in the nanomolar range. Quisinostat was the most potent with an EC50 of 4.5 nM. It was observed that unsaturated and aryl hydroxamic acids were more inhibitory than saturated vorinostat and that hydroxamic acids in general had more potent EC50s than did the benzamides mocetinostat and entinostat.

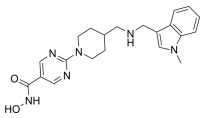
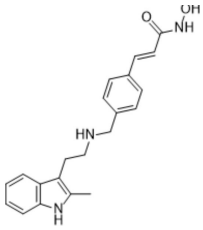
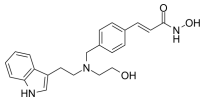
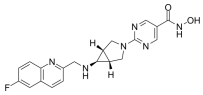
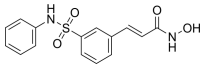
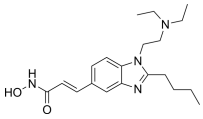
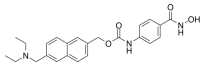
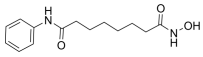
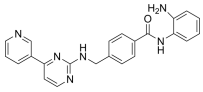
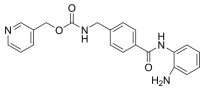
Cytotoxicity testing

Basic cytotoxicity testing of HDAC inhibitors was performed in human HCT8 cells as described above. Results are reported in Table 1. HDAC inhibitor compounds did show toxicity in human HCT8 cells, but at concentrations significantly higher than what was required for inhibition of *B. duncani*. For example, while the compound most toxic to HCT8 cells appeared to be nanatinostat, which had an EC50 of 56.25 µM, by contrast, its EC50 of 23 nM in *B. duncani* was 2,400× lower.

DISCUSSION

Effective treatment for human babesiosis is a public health concern of growing significance (22). *In vitro* testing of recommended therapies in *B. duncani* shows that of the four drugs used in clinical practice, only atovaquone would be considered significantly inhibitory, with an EC50 of 517 nM. In the effort to discover new antimicrobials

TABLE 1 EC50s and cytotoxicity of select histone deacetylase inhibitors[a]

Compound	EC50 (µM)	95% CI EC50 (µM)	TC50 HCT8 (µM)	95% CI TC50 (µM)	Therapeutic index
Quisinostat	0.0045	0.0039–0.0051	170	120–380	38,000
					
Panobinostat	0.0084	0.0054–0.013	130	34–340	16,000
					
Dacinostat	0.023	0.021–0.026	150	120–270	6,600
					
Nanatinostat	0.024	0.021–0.027	44	40–49	1,900
					
Belinostat	0.15	0.12–0.18	90	61–120	600
					
Pracinostat	0.16	0.14–0.18	450	Wide	2,800
					
Givinostat	0.22	0.19–0.26	43	31–57	190
					
Vorinostat	1.1	0.98–1.2	No toxicity	Wide	NA[b]
					
Mocetinostat	2.5	2.0–3.0	56	Wide	23
					
Entinostat	23	20–26	110	95–170	5
					

[a]Compounds are arranged by inhibitory potency against *B. duncani* with the most potent on top. Dose response in *Babesia was* performed with two replicate 9-point dilution experiments with combined data reported. Toxicity studies were performed on confluent monolayer HCT8 cells using the Promega CellTiter Aqueous One Solution Cell Proliferation Assay, with two replicate experiments per compound, and the combined data were reported.
[b]NA, A therapeutic index could not be calculated for vorinostat, as no toxicity was detected at the measured drug concentrations.

and druggable targets, a high-throughput screening assay, which is both cheaper and more efficient, will be an invaluable tool. The assay described above uses a new parasite

staining method and miniaturized culture conditions, and its Z′-score of 0.82 indicates its utility for library screening.

Using this assay, we have obtained EC50 results similar to those reported by other researchers. Our atovaquone EC50 of 517 nM is consistent with reporting from Abraham et al., who arrived at an EC50 of 500 nm in *Babesia duncani* using the SYBR green assay (9). We note that later *Babesia duncani* testing reported by different authors (but the same lab group) found a substantially lower atovaquone EC50 of 72 nM (23). It is unclear to us whether this represents the use of a different *B. duncani* isolate or a change in methods.

PI ($104/10 mL Fisher P3566) is much less expensive than SYBR green ($96.00/400 µL Fisher S33102). Previous assays have only described a fluorescence-based technique in 96-well plates (14–16). Our assay uses 384-well plates, which allow for (i) smaller amounts of reagent/experiment and (ii) a higher number of potential samples or replicates/experiment. These two factors make this assay more efficient and less expensive to run than prior established techniques. The use of PI and the miniaturized culture format of 384-well plates will, therefore, minimize the cost of reagents and the quantity of compounds required for screening and *in vitro* follow-up, making this method an attractive alternative to those previously reported (9, 14–16). This assay's utility in practice is demonstrated by its deployment in a screen of the SGC Bug Box compound collection with a yield of both known and novel compounds inhibitory to *Babesia duncani*.

Diphenyleneiodonium chloride (DPI) is believed to inhibit NADP/NADPH oxidase and has been identified as an inhibitor of *M. tuberculosis, S. aureus*, and multiple species of non-Tuberculous mycobacteria (24, 25). One study synthesized two series of DPI analogs and showed good activity against *P. falciparum*; however, significant concerns around cytotoxicity were noted (26). To the best of our knowledge, this is the first time this compound has been identified as an *in vitro* inhibitor of *Babesia*. There are currently no published human trials with DPI. While this certainly may represent a potential chemical structure and/or target for further pursuit, the apparent lack of further progress in the development of this compound for clinical use suggests that there are significant obstacles to its study.

Trimethoprim and SDDC-M7 are both thought to target parasite dihydrofolate reductase (DHFR), a critical enzyme for tetrahydrofolate synthesis required for the synthesis of purines and some amino acids. Control compound WR99210 also targets DHFR (27, 28), and this drug target has been extensively studied and described in *Babesia* and other parasites (20). Unfortunately, SDDC-M7 is not commercially available, and the researchers who originally synthesized it could not be contacted; thus, further study of this hit compound by our group was not possible.

The molecular target of panobinostat is believed to be a family of epigenetic modification enzymes called histone deacetylase complexes. Panobinostat has been approved as an oral treatment for multiple myeloma, and other HDAC inhibitors have been used for numerous forms of both solid organ and hematologic malignancy (29). There are 18 mammalian HDACs, which are divided into two families: the histone deacetylase family and the sirtuin protein family (30). Panobinostat is considered a nonselective inhibitor within the histone deacetylase family. While its known activity in human cells (and role as a chemotherapy agent) could be considered a red flag, prior studies have shown that panobinostat's cytotoxicity is fairly selective for malignant cells, possibly because HDACs are relatively more expressed in this cell population (31). While panobinostat LD90s have been reported as less than 500 nM for solid tumor cells and less than 100 nM for liquid tumor cell lines, testing in normal cell lines (human mammary and renal epithelial cells, among others) has shown LD90s > 5 µM. Similarly, while malignant cells treated with panobinostat had a 10- to 11-fold increase in apoptotic signaling, normal cells showed no increase in caspase expression compared with control (32). Cardiac toxicity has been an issue in this drug class; however, medicinal chemistry

optimization approaches have successfully yielded compound derivatives that mitigate this problem (21).

HDAC inhibitors have also been explored for therapeutic applications against intracellular parasites, including other Apicomplexa such as *P. falciparum* and *T. gondii,* with some displaying good selectivity for parasite over host cells and even activity against drug-resistant *P. falciparum* (33). While apicidin has been shown to have inhibitory activity on *B. bovis* (34), and a screen of epigenetic modifying compounds showed inhibitory activity of HDAC inhibitors in *Babesia divergens*, it does not appear that such compounds have previously been tested in *Babesia duncani* (35).

Our HDAC inhibitor testing corroborates Vanheer et al., who performed dose-response testing of HDAC inhibitors in *B. divergens* with EC50 values similar to those we found in *Babesia duncani*, and with potency trends preserved. Dacinostat, panobinostat, and quisinostat had EC50s of 111.9, 27.2, and 4.6 nM in *B. divergens* and 23, 8, and 4.5 nM in *B. duncani* (35). Panobinostat and quisinostat are quite potent in *P. falciparum* as well, with EC50s of 10–30 nM and 5–7 nM depending on the strain tested (36, 37).

From a chemistry perspective, most of the HDAC inhibitors evaluated, including compounds panobinostat, vorinostat, belinostat, and dacinostat, are hydroxamic acids, while entinostat and mocetinostat are benzamides (38). Our early-stage SAR indicates that the hydroxamic acids have greater inhibitory activity against *B. duncani* than do the benzamides. The greater anti-*Babesia* potency of the hydroxyamic acids vs benzamides may be related to differences in target selectivity since the benzamides entinostat and mocetinostat inhibit only class I or class I and II HDAC, respectively, while many of the remaining compounds are pan-HDAC inhibitors (39–42). Another general trend we observe is that saturation of the hydroxamic acid (i.e., vorinostat) seems to result in a reduction of potency.

Of the HDAC inhibitor compounds tested, quisinostat and nanatinostat are of particular interest. Both have excellent potency (EC50s 4.5 and 23.8 nM, respectively). While many compounds of the series contain an a,b-unsaturated hydroxamic acid, a potential Michael acceptor, concerning for indiscriminate reactivity, aryl hydroxamic acids quisinostat and nanatinostat both lack this feature, which may mitigate some toxic potential. It is worth noting that both compounds are orally bioavailable and have been the subject of phase I and II trials in humans; thus, data on pharmacodynamic, pharmacokinetic, and toxic characteristics in humans are available.

Quisinostat is a second-generation hydroxamic acid-based pan-HDAC inhibitor (active in HDAC classes I, II, and IV) (39); however, it is reported to be selective for HDAC class I when given in low doses (43). Its *in vitro* IC90 for *B. duncani* is 10 nM, which is equivalent to a free plasma concentration of approximately 4 ng/mL. Clinical data indicate that a peak plasma concentration (Cmax) of 1.9 ng/mL and area under the curve (AUC) of 18 ng*H/mL can be achieved with a dosing strategy of 12 mg given orally (PO) thrice weekly, and with minimal side effects (43). While the Cmax appears unimpressive, it is quite possible that even with such low doses, the AUC is adequate for clearance of parasitemia. Given that this dosing is a conservative approach toward mitigating toxicity for prolonged use (i.e., as chemotherapy for cancer), one could, moreover, dose this drug much more aggressively in the context of acute babesiosis treatment, which would be expected to last only 7–10 days.

Nanatinostat is thought to be selective for HDAC class I, surprising given that its potency is comparable to the pan-HDAC inhibitors. Its IC90 against *B. duncani* was found to be 64 nM, equivalent to a free plasma concentration of approximately 25 ng/mL, while 3× EC50 would be approximately 28 ng/mL. Clinical data indicate that a Cmax of 186 ng/mL can be achieved with a single 20 mg oral dose (44). With a single 80 mg oral dose, the protocol defined maximum tolerated dose (28-day, once-daily dosing study in humans), plasma concentrations remain above the *B. duncani* IC90 for nearly 12 hours (45). It remains to be seen whether Babesia inhibition is dependent on time above MIC, AUC, or maximum serum drug concentration or if multiple doses per day are tolerable in humans.

Since the growth of *Babesia* within erythrocytes is likely independent of host HDACs, quisinostat and nanatinostat likely work by inhibiting one or more *B. duncani* HDAC or, less likely, through a completely off-target mechanism. Based on the BLAST search using human HDAC 8 (the most established target of quisinostat), four possible HDACs are encoded in the *B. duncani* genome. The most closely related *B. duncani* HDAC (BdWA1_002946) is conserved in the main human pathogens *B. microti* and *B. divergens* with 88% and 94% amino acid identity (96% and 97% similarity) in the known quisinostat-binding pocket (46). On the other hand, sequence identity and similarity to human HDAC8 are 66% and 81%, respectively. This could partially explain the exceptionally high therapeutic index observed with these compounds, and in the case that toxicity limits the direct repurposing of quisinostat or nanatinostat to treat Babesiosis, could offer opportunities for target-based optimization.

Limitations and future directions

This work is illustrative of the value provided by an improved high-throughput drug screening assay for *Babesia duncani*. The logical next step is to use it much more widely for the screening of other compound libraries. A truly unbiased screening of compound libraries (i.e., those with a population predominantly non-inhibitory to the parasite) would allow for calculation of a Z score to characterize the performance of the PI-based assay in practice (not to be confused with the Z′ score calculated herein using controls and background) (19). This could not be done from screening of the Bug Box because it was a collection of compounds with known antimicrobial activity, hence with a rather high pretest probability of inhibitory activity. We are currently screening several compound series known to have activity in Apicomplexa and larger, unbiased compound libraries. This should allow both for the discovery of new hit compounds and for a Z score calculation.

The toxicity studies pursued herein were limited to a single cell line, given that the inhibitors identified have undergone so much human clinical and preclinical development already. We note that HCT8 cells seem to have been remarkably resilient to the effect of panobinostat compared with other colon cancer cell lines tested in the past (47). We hypothesize that this is due to the culture method we use of growing HCT8 cells to a confluent monolayer before exposing them to the drug. Perhaps as a result of having reached confluence, the HCT8 cells were relatively metabolically inert during drug exposure and hence less sensitive to its effects (expected to be most profound in rapidly dividing cells).

This screen of the Bug Box represents a proof of concept for the effectiveness of our new drug screening assay. To move from assay hits to true lead compounds, we would need to perform target validation and also assess drug effectiveness and safety in an animal model of disease. A murine model of *Babesia duncani* has already been described (17); thus, further evaluation of hits, including the HDAC inhibitor series, should be a relatively straightforward enterprise. While it is a good thought experiment to consider whether the *in vitro* data and human PK data suggest that quisinostat and nanatinostat have potential for human anti-Babesia drugs, a study in mice will clearly be a necessary bridging step to define PK/PD relative to the MTD in humans.

MATERIALS AND METHODS

Culture maintenance and culture preparation for compound screening

Frozen stocks of *B. duncani* were provided by the Ben Mamoun lab at Yale University. Culture maintenance was undertaken as described by Singh et al[18] with the following adaptations: Media, completed DMEM/F12 (cDMEM; 20% heat-inactivated fetal bovine serum (Sigma-Aldrich catalogue #12,306 C-500ML), 1 x HT media supplement (Sigma-Aldrich catalogue # H0137-10VL), 1 x L-glutamine (Gibco, catalogue # 25030–081), 1 x antibiotic-antimycotic (Gibco catalogue #15240–062), and 1 x gentamicin (Gibco

catalogue #15710–072)), was changed every other day and cultures were kept in a modular incubator gassed with 2% O_2, 5% CO_2, 93% N_2 at 37°C. Passage occurred once a week into fresh blood at 1%–2% parasitemia, 5% hematocrit, and fresh A + blood was obtained once a week from the University of Vermont Medical Center Blood Bank. Four days before the start of drug assay testing, a 10 mL, 5% hematocrit culture was infected to 2% parasitemia with *Babesia duncani*. One day before the start, the media was changed, and parasitemia was assessed by light microscopy examination of Giemsa-stained thin blood smears with a minimum of 500 red blood cells counted.

Experimental compounds

The following compounds were purchased from the respective supplier: Atovaquone (Thermo Scientific, catalog #468762500); Azithromycin (Tokyo Chemical Industry (TCI), catalog #A2076); Clindamycin (TCI, catalog #C2257); Quinine (TCI, catalog # Q0028); and WR99210 (Sigma, catalog #SML2976). The Bug Box compounds were provided by the Structural Genomics Consortium/University of Toronto. Hit compounds and structurally similar series were then purchased from MedChemExpress for dose-response assays (catalog #HY-100965, #HY-10224, #HY-B0510, #HY-12163, #HY-10221, #HY-14842, #HY-13322, #HY-12164, #HY-13432, and #HY-15433).

Diluting parasitemia experiments

Fresh A + blood was washed three times, and a stock 10% hematocrit (HCT) solution of uninfected red cells in completed F12/DMEM media (cDMEM) was created. In a 96-well plate, a pellet from a vigorously growing (≥20% parasitemia) culture was used to create a 10% hematocrit starting well that was then serially diluted five times with the stock 10% hematocrit solution. 25 µL of each serial dilution was transferred to a white, clear-bottom 384-well plate (Falcon, catalog #353963) in triplicate before 25 µL of cDMEM was added to each well, followed by 25 µL of 0.6% Triton-X, 22.5 µM PI in phosphate-buffered solution. The 384-well plate was then shaken for 30 seconds, incubated at 37°C for 1 hour (in the dark), then moved to room temperature in the dark. After 24 hours, the plate was read using a Synergy H1 (BioTek, Winooski, VT) with excitation = 535 nm, emission = 615 nm, sensitivity = 150, and readings taken from the bottom of the wells. Blood smears were made from select undiluted starting wells and stained with Giemsa, and parasitemia was calculated manually from a minimum of 1,000 counted red blood cells. The experiment was repeated twice.

Growth kinetics experiments

Experiments were performed to compare the growth of *B. duncani* in 96-well and 384-well plates. For 96-well plates, a nine-point serial dilution of parasitemia was made as described above, and infected erythrocytes were then seeded into a 96-well plate and incubated for 48 hours. The final hematocrit for the experiment was 5%. Blood smears were made for each point of serial dilution at both time zero and the 48 hour mark. Smears were stained with Giemsa, and parasites were counted. Parasitemia was calculated with a minimum of 1,000 cells counted per slide. For 384-well plates, *B. duncani*-infected red blood cells were seeded into 384-well plates at a starting parasitemia of 7.5%. At time points of 24 hours, 30 hours, 48 hours, and 72 hours, parasitemia was monitored with both blood smears/manual parasite counting and PI staining and plate reading. Separate plates were used for each of the five time points. PI staining and fluorimetry of the time zero point included 22 wells, the 24 hour time point included 28 wells, and all others were 27-well technical replicates.

Z′ score experiments and Calculation

To calculate the Z′ score, half of a 384-well plate (154 wells) was plated with *B. duncani*-infected RBCs (5% parasitemia) and treated with WR99210 (dissolved in DMSO, diluted

with cDMEM) to a final concentration of 25 µM drug, 5% HCT. The other half plate was likewise infected and treated with 0.5% DMSO (final 0.25% DMSO) in cDMEM. The plate was incubated for 48 hours, stained with propidium iodide, and read as described above.

Z′ scores for the assay were calculated using the described equation in Zhang et al., 1999[15] seen below.

$$Z' = \frac{3 \cdot \sigma_{\text{Infected wells}} + 3 \cdot \sigma_{\text{Treated Infected wells}}}{\left|\mu_{\text{Infected wells}} + \mu_{\text{Treated Infected wells}}\right|}$$

Compound testing

Prior to the removal of the culture(s) from the modular incubator, fresh A + blood was washed three times with PSG +and compounds (in DMSO stocks) to be tested were prepared in a 96-well plate by serial dilution in cDMEM. Once prepared, the culture(s) were removed from the modular incubator, collected, and washed once with 7 mL of cDMEM. A 10% hematocrit, 5% parasitemia stock in cDMEM was made, and 25 µL aliquoted into a 384-well plate with constant agitation, followed by 25 µL of compound dilution (quadruplicates). The positive growth control was given 25 µL of 0.5% dimethyl sulfoxide (DMSO) in cDMEM (final 0.25% DMSO), and the negative growth control was 25 µL of 50 µM WR99210 (0.5% DMSO) (final 25 µM WR99210, 0.25% DMSO). Plates were incubated as previously described, smears of the positive growth control were made, and the plates were read as previously described. Smears were stained by Giemsa, and a minimum of 1,000 RBCs were counted to determine parasitemia. Dose-response assays were repeated twice.

Pilot dose-response experiments were performed using WR99210 (a DHFR inhibitor with known effect on Babesia duncani), DMSO vehicle, and standard of care drugs atovaquone, clindamycin, quinine, and azithromycin (20). During initial experiments, positive growth control wells (infected red blood cells) were treated with 0.25% DMSO in cDMEM with a background subtraction factor established using averaged wells containing uninfected red blood cells and % inhibition calculated using the formula:

$$\%\ \text{inhibition} = 100 \times [(\ \text{positive growth control} - \text{x})/(\ \text{positive growth control}\ )]$$

We independently established the potency of WR99210 (~8.3 nM) and then adopted the practice of using this compound as a negative growth control (minimum) in place of uninfected red blood cells. The positive growth control was treated with 25 µL of 0.5% dimethyl sulfoxide (DMSO) in cDMEM (final 0.25% DMSO), and the negative growth control with 25 µL of 50 µM WR99210 (0.5% DMSO) (final 25 µM WR99210, 0.25% DMSO). The plate was incubated for 48 hours and then the plate was stained and read as previously described. RFUs from positive and negative growth control wells were averaged (n = 27). % inhibition calculation was changed to:

$$\%\ \text{inhibition} = 100\ [(\text{max-x})/(\text{max-min})]$$

OR

$$\%\text{inhibition} = 100 \times [(\text{positive growth control} - \text{x})/ (\text{positive growth control–negative growth control})]$$

"Bug Box" compound series screen and validation

The Bug Box is a collection of 40 compounds with known antimicrobial and/or bioactivity, which was provided by the Structural Genomics Consortium (SGC)-Toronto. The full list of compounds is available in the supplement. They were obtained in 10 mM aliquots and screened in 384-well plates at 1 µM and 5 µM dilutions with four technical replicates per dilution. Hits were defined as those compounds with at least 80% inhibition. Hits were validated by dose-response curves using commercially obtained compounds

with verified purity. The only exception to this was in the verification of compound M7, which is a proprietary compound that could be obtained only from SGC-Toronto. Dose-response curves were created from two independent experiments, each with nine dilutions of the drug. Panobinostat and its putative target, the histone deacetylase complex, were selected for further study, with dose-response curves generated for nine structurally similar compounds in an effort to evaluate structure-activity relationships (SARs).

Cytotoxicity assays

Human HCT8 cells were grown in tissue culture flasks until a confluent monolayer was achieved. Cells were then transferred to 384-well plates, where they were again grown into a confluent monolayer (approximately 48 hours of incubation). 9-point dilutions of lead compounds were prepared in 96-well plates (highest concentration 200 µM for final concentration 100 µM) and then added in a 1:1 ratio to 384-well plates containing HCT8 cells. Cells were incubated with the drug for 48 hours. Promega CellTiter Aqueous One Solution Cell Proliferation Assay (MTS) (PRG3580) was commercially obtained and used to ascertain cell viability, with luminescence measured using a Biotek microplate reader. Cells incubated in 0.5% DMSO served as a positive growth control and comparator arm.

Data handling and analysis

The raw relative fluorescent units (RFU) output from Gen5 version 1.11 were imported into Microsoft Excel for data organization and analysis. GraphPad Prism version 10.0.2 (GraphPad Software, San Diego, CA) was used to generate dose-response curves (see below) and graphs.

To generate the simple linear regression, Prism default settings were used along with the option to consider each replicate Y value as an individual point.

To generate dose-response curves, % inhibition from each experimental well was calculated as described above, and then % inhibition from the four replicate wells (for each compound dilution) was averaged. Each experiment was repeated at least twice, with EC50 values derived from the combination of the two data sets generated. EC_{50} values were calculated in GraphPad Prism as per the following equation, with the top constrained to 100: $Y = Bottom + (Top - Bottom)/(1 + 10^{LogEC50} - X \times Hill\ slope)$, where Y is the percent inhibition, X is the drug concentration, and Hill slope is the largest absolute value of the slope of the curve.

ACKNOWLEDGMENTS

The compound library screened ("Bug Box") was provided by the Structural Genomics Consortium-Toronto. Red blood cells used in culture of *Babesia duncani* were provided by the University of Vermont Medical Center Blood Bank. We acknowledge the assistance of Dr. Choukri Ben Mamoun and Dr. Pallavi Singh at Yale University who provided frozen stocks of *Babesia duncani* and protocols for continuous *in vitro* culture.

Support for this project was provided by the University of Vermont Larner College of Medicine Internal Grant Program and by the Translational Global Infectious Diseases Research Center of Biomedical Excellence Pilot Award Grant which is funded by the National Institutes of Health (NIH) award number P20 GM125498.

AUTHOR AFFILIATIONS

[1]Department of Medicine, University of Vermont Larner College of Medicine, Burlington, Vermont, USA
[2]Department of Microbiology and Molecular Genetics Master's Program, University of Vermont, Burlington, Vermont, USA

[3]Cell, Molecular, and Biomedical Sciences Graduate Program, University of Vermont, Burlington, Vermont, USA
[4]Department of Chemistry, Saint Louis University, St. Louis, Missouri, USA

PRESENT ADDRESS

Emmett A. Dews, University of Texas-Galveston Medical Branch, Galveston, Texas, USA

AUTHOR ORCIDs

Peter R. Hyson http://orcid.org/0000-0002-8810-1230

AUTHOR CONTRIBUTIONS

Emmett A. Dews, Conceptualization, Data curation, Formal analysis, Investigation, Methodology, Validation, Writing – review and editing | José E. Teixeira, Conceptualization, Methodology, Supervision, Validation, Writing – review and editing | Christopher D. Huston, Conceptualization, Funding acquisition, Supervision, Writing – review and editing | Marvin J. Meyers, Conceptualization, Writing – review and editing | Peter R. Hyson, Conceptualization, Data curation, Formal analysis, Funding acquisition, Investigation, Methodology, Project administration, Resources, Supervision, Validation, Visualization, Writing – original draft, Writing – review and editing

DATA AVAILABILITY

By publishing in the journal, the authors agree that, subject to requirements or limitations imposed by local and/or U.S. Government laws and regulations, any materials and data that are reasonably requested by others are available from a publicly accessible collection or will be made available in a timely fashion, at reasonable cost, and in limited quantities to members of the scientific community for noncommercial purposes.

ADDITIONAL FILES

The following material is available online.

Supplemental Material

Fig. S1 (AAC00035-25-s0001.tif). Screened compounds from "Bug Box".

REFERENCES

1. Gray EB, Herwaldt BL. 2019. Babesiosis surveillance - United States, 2011-2015. MMWR Surveill Summ 68:1–11. https://doi.org/10.15585/mmwr.ss6806a1
2. Kumar A, O'Bryan J, Krause PJ. 2021. The global emergence of human babesiosis. Pathogens 10:1447. https://doi.org/10.3390/pathogens10111447
3. Wallace BI, Kenney B, Malani PN, Clauw DJ, Nallamothu BK, Waljee AK. 2021. Prevalence of immunosuppressive drug use among commercially insured US adults, 2018-2019. JAMA Netw Open 4:e214920. https://doi.org/10.1001/jamanetworkopen.2021.4920
4. Vannier E, Krause PJ. 2012. Human babesiosis. N Engl J Med 366:2397–2407. https://doi.org/10.1056/NEJMra1202018
5. Lantos PM, Rumbaugh J, Bockenstedt LK, Falck-Ytter YT, Aguero-Rosenfeld ME, Auwaerter PG, Baldwin K, Bannuru RR, Belani KK, Bowie WR, et al. 2021. Clinical practice guidelines by the infectious diseases society of America, American academy of neurology, and American college of rheumatology: 2020 guidelines for the prevention, diagnosis, and treatment of lyme disease. Neurology (ECronicon) 96:262–273. https://doi.org/10.1212/WNL.0000000000011151
6. Krause PJ, Gewurz BE, Hill D, Marty FM, Vannier E, Foppa IM, Furman RR, Neuhaus E, Skowron G, Gupta S, et al. 2008. Persistent and relapsing babesiosis in immunocompromised patients. Clin Infect Dis 46:370–376. https://doi.org/10.1086/525852
7. Wormser GP, Prasad A, Neuhaus E, Joshi S, Nowakowski J, Nelson J, Mittleman A, Aguero-Rosenfeld M, Topal J, Krause PJ. 2010. Emergence of resistance to azithromycin-atovaquone in immunocompromised patients with *Babesia microti* infection. Clin Infect Dis 50:381–386. https://doi.org/10.1086/649859
8. Marcos LA, Leung A, Kirkman L, Wormser GP. 2022. Use of tafenoquine to treat a patient with relapsing babesiosis with clinical and molecular evidence of resistance to azithromycin and atovaquone. IDCases 27:e01460. https://doi.org/10.1016/j.idcr.2022.e01460
9. Abraham A, Brasov I, Thekkiniath J, Kilian N, Lawres L, Gao R, DeBus K, He L, Yu X, Zhu G, Graham MM, Liu X, Molestina R, Ben Mamoun C. 2018. Establishment of a continuous *in vitro* culture of *Babesia duncani* in human erythrocytes reveals unusually high tolerance to recommended therapies. J Biol Chem 293:19974–19981. https://doi.org/10.1074/jbc.AC118.005771
10. Agarwal P, Anvikar AR, Pillai CR, Srivastava K. 2017. *In vitro* susceptibility of Indian *Plasmodium falciparum* isolates to different antimalarial drugs & antibiotics. Indian J Med Res 146:622–628. https://doi.org/10.4103/ijmr.IJMR_1688_15
11. Matsubara J, Koura M, Kamiyama T. 1993. Infection of immunodeficient mice with a mouse-adapted substrain of the gray strain of *Babesia microti*. J Parasitol 79:783–786. https://doi.org/10.2307/3283623

12. Gray JS, Pudney M. 1999. Activity of atovaquone against *Babesia microti* in the Mongolian gerbil, *Meriones unguiculatus*. J Parasitol 85:723–728. https://doi.org/10.2307/3285750
13. Rubin LG, Schaffner W. 2014. Clinical practice. Care of the asplenic patient. N Engl J Med 371:349–356. https://doi.org/10.1056/NEJMcp1314291
14. Rizk MA, El-Sayed S-S, Terkawi MA, Youssef MA, El Said E, Elsayed G, El-Khodery S, El-Ashker M, Elsify A, Omar M, Salama A, Yokoyama N, Igarashi I. 2015. Optimization of a fluorescence-based assay for large-scale drug screening against *Babesia* and *Theileria* parasites. PLoS ONE 10:e0125276. https://doi.org/10.1371/journal.pone.0125276
15. Rizk MA, El-Sayed S-S, AbouLaila M, Tuvshintulga B, Yokoyama N, Igarashi I. 2016. Large-scale drug screening against *Babesia divergens* parasite using a fluorescence-based high-throughput screening assay. Vet Parasitol 227:93–97. https://doi.org/10.1016/j.vetpar.2016.07.032
16. Guswanto A, Sivakumar T, Rizk MA, Elsayed SAE, Youssef MA, ElSaid EES, Yokoyama N, Igarashi I. 2014. Evaluation of a fluorescence-based method for antibabesial drug screening. Antimicrob Agents Chemother 58:4713–4717. https://doi.org/10.1128/AAC.00022-14
17. Pal AC, Renard I, Singh P, Vydyam P, Chiu JE, Pou S, Winter RW, Dodean R, Frueh L, Nilsen AC, Riscoe MK, Doggett JS, Ben Mamoun C. 2022. *Babesia duncani* as a model organism to study the development, virulence, and drug susceptibility of intraerythrocytic parasites *in vitro* and *in vivo*. J Infect Dis 226:1267–1275. https://doi.org/10.1093/infdis/jiac181
18. Vinayak S, Jumani RS, Miller P, Hasan MM, McLeod BI, Tandel J, Stebbins EE, Teixeira JE, Borrel J, Gonse A, et al. 2020. Bicyclic azetidines kill the diarrheal pathogen *Cryptosporidium* in mice by inhibiting parasite phenylalanyl-tRNA synthetase. Sci Transl Med 12:eaba8412. https://doi.org/10.1126/scitranslmed.aba8412
19. Zhang JH, Chung TD, Oldenburg KR. 1999. A simple statistical parameter for use in evaluation and validation of high throughput screening assays. J Biomol Screen 4:67–73. https://doi.org/10.1177/108705719900400206
20. Singh P, Lonardi S, Liang Q, Vydyam P, Khabirova E, Fang T, Gihaz S, Thekkiniath J, Munshi M, Abel S, et al. 2023. *Babesia duncani* multi-omics identifies virulence factors and drug targets. Nat Microbiol 8:845–859. https://doi.org/10.1038/s41564-023-01360-8
21. Shultz MD, Cao X, Chen CH, Cho YS, Davis NR, Eckman J, Fan J, Fekete A, Firestone B, Flynn J, et al. 2011. Optimization of the *in vitro* cardiac safety of hydroxamate-based histone deacetylase inhibitors. J Med Chem 54:4752–4772. https://doi.org/10.1021/jm200388e
22. Swanson M, Pickrel A, Williamson J, Montgomery S. 2023. Trends in reported babesiosis cases - United States, 2011-2019. MMWR Morb Mortal Wkly Rep 72:273–277. https://doi.org/10.15585/mmwr.mm7211a1
23. Chiu JE, Renard I, Pal AC, Singh P, Vydyam P, Thekkiniath J, Kumar M, Gihaz S, Pou S, Winter RW, Dodean R, Frueh L, Nilsen AC, Riscoe MK, Doggett JS, Mamoun CB. 2021. Effective therapy targeting cytochrome bc_1 prevents *Babesia* erythrocytic development and protects from lethal infection. Antimicrob Agents Chemother 65:e0066221. https://doi.org/10.1128/AAC.00662-21
24. Pandey M, Singh AK, Thakare R, Talwar S, Karaulia P, Dasgupta A, Chopra S, Pandey AK. 2017. Diphenyleneiodonium chloride (DPIC) displays broad-spectrum bactericidal activity. Sci Rep 7:11521. https://doi.org/10.1038/s41598-017-11575-5
25. Singh AK, Thakare R, Karaulia P, Das S, Soni I, Pandey M, Pandey AK, Chopra S, Dasgupta A. 2017. Biological evaluation of diphenyleneiodonium chloride (DPIC) as a potential drug candidate for treatment of non-tuberculous mycobacterial infections. J Antimicrob Chemother 72:3117–3121. https://doi.org/10.1093/jac/dkx277
26. Nguyen N, Wilson DW, Nagalingam G, Triccas JA, Schneider EK, Li J, Velkov T, Baell J. 2018. Broad activity of diphenyleneiodonium analogues against *Mycobacterium tuberculosis*, malaria parasites and bacterial pathogens. Eur J Med Chem 148:507–518. https://doi.org/10.1016/j.ejmech.2017.10.010
27. Gleckman R, Blagg N, Joubert DW. 1981. Trimethoprim: mechanisms of action, antimicrobial activity, bacterial resistance, pharmacokinetics, adverse reactions, and therapeutic indications. Pharmacotherapy 1:14–20. https://doi.org/10.1002/j.1875-9114.1981.tb03548.x
28. Mayclin SJ, Fairman JW, Dranow DM, Conrady DG, Lukacs CM, Lorimer DD, Horanyi PS, Edwards TE, Abendroth J. 2021. Crystal structure of dihydrofolate reductase from *Mycobacterium tuberculosis* bound to NADP and SDDC inhibitor SDDC-M7. Available from: https://doi.org/10.2210/pdb5SCO/pdb
29. Eckschlager T, Plch J, Stiborova M, Hrabeta J. 2017. Histone deacetylase inhibitors as anticancer drugs. Int J Mol Sci 18:1414. https://doi.org/10.3390/ijms18071414
30. Park S-Y, Kim J-S. 2020. A short guide to histone deacetylases including recent progress on class II enzymes. Exp Mol Med 52:204–212. https://doi.org/10.1038/s12276-020-0382-4
31. El Omari N, Bakrim S, Khalid A, Abdalla AN, Almalki WH, Lee L-H, Ardianto C, Ming LC, Bouyahya A. 2023. Molecular mechanisms underlying the clinical efficacy of panobinostat involve Stochasticity of epigenetic signaling, sensitization to anticancer drugs, and induction of cellular cell death related to cellular stresses. Biomed Pharmacother 164:114886. https://doi.org/10.1016/j.biopha.2023.114886
32. Atadja P. 2009. Development of the pan-DAC inhibitor panobinostat (LBH589): successes and challenges. Cancer Lett 280:233–241. https://doi.org/10.1016/j.canlet.2009.02.019
33. Mohapatra TK, Nayak RR, Ganeshpurkar A, Tiwari P, Kumar D. 2024. Opportunities and difficulties in the repurposing of HDAC inhibitors as antiparasitic agents. DDC 3:70–101. https://doi.org/10.3390/ddc3010006
34. Munkhjargal T, Aboulaila M, Ueno A, Sivakumar T, Nakano Y, Yokoyama M, Yokoyama N, Igarashi I. 2012. Cloning and characterization of histone deacetylase from *Babesia bovis*. Vet Parasitol 190:423–433. https://doi.org/10.1016/j.vetpar.2012.06.026
35. Vanheer LN, Kafsack BFC. 2021. Activity comparison of epigenetic modulators against the hemoprotozoan parasites *Babesia divergens* and *Plasmodium falciparum*. ACS Infect Dis 7:2277–2284. https://doi.org/10.1021/acsinfecdis.0c00853
36. Engel JA, Jones AJ, Avery VM, Sumanadasa SDM, Ng SS, Fairlie DP, Skinner-Adams T, Andrews KT. 2015. Profiling the anti-protozoal activity of anti-cancer HDAC inhibitors against *Plasmodium* and *Trypanosoma parasites*. Int J Parasitol Drugs Drug Resist 5:117–126. https://doi.org/10.1016/j.ijpddr.2015.05.004
37. Li R, Ling D, Tang T, Huang Z, Wang M, Ding Y, Liu T, Wei H, Xu W, Mao F, Zhu J, Li X, Jiang L, Li J. 2021. Discovery of novel *Plasmodium falciparum* HDAC1 inhibitors with dual-stage antimalarial potency and improved safety based on the clinical anticancer drug candidate quisinostat. J Med Chem 64:2254–2271. https://doi.org/10.1021/acs.jmedchem.0c02104
38. Subramanian S, Bates SE, Wright JJ, Espinoza-Delgado I, Piekarz RL. 2010. Clinical toxicities of histone deacetylase inhibitors. Pharmaceuticals (Basel) 3:2751–2767. https://doi.org/10.3390/ph3092751
39. Morales Torres C, Wu MY, Hobor S, Wainwright EN, Martin MJ, Patel H, Grey W, Grönroos E, Howell S, Carvalho J, Snijders AP, Bustin M, Bonnet D, Smith PD, Swanton C, Howell M, Scaffidi P. 2020. Selective inhibition of cancer cell self-renewal through a Quisinostat-histone H1.0 axis. Nat Commun 11:1792. https://doi.org/10.1038/s41467-020-15615-z
40. Briere D, Sudhakar N, Woods DM, Hallin J, Engstrom LD, Aranda R, Chiang H, Sodré AL, Olson P, Weber JS, Christensen JG. 2018. The class I/IV HDAC inhibitor mocetinostat increases tumor antigen presentation, decreases immune suppressive cell types and augments checkpoint inhibitor therapy. Cancer Immunol Immunother 67:381–392. https://doi.org/10.1007/s00262-017-2091-y
41. Looi C-K, Gan L-L, Sim W, Hii L-W, Chung F-L, Leong C-O, Lim W-M, Mai C-W. 2022. Histone deacetylase inhibitors restore cancer cell sensitivity towards T lymphocytes mediated cytotoxicity in pancreatic cancer. Cancers (Basel) 14:3709. https://doi.org/10.3390/cancers14153709
42. Novotny-Diermayr V, Sausgruber N, Loh YK, Pasha MK, Jayaraman R, Hentze H, Yong WP, Goh BC, Toh HC, Ethirajulu K, Zhu J, Wood JM. 2011. Pharmacodynamic evaluation of the target efficacy of SB939, an oral HDAC inhibitor with selectivity for tumor tissue. Mol Cancer Ther 10:1207–1217. https://doi.org/10.1158/1535-7163.MCT-11-0044
43. Cascio CL, Margaryan T, Melendez EL, McNamara JB, White CI, Knight W, Ganta S, Opachich Z, Yoo W, Sanai N, Tovmasyan A, Mehta S. 2022. Quisinostat is a brain-penetrant radiosensitizer in glioblastoma. bioRxiv. https://doi.org/10.1101/2022.11.09.515859:2022.11.09.515859
44. Haverkos B, Alpdogan O, Baiocchi R, Brammer JE, Feldman TA, Capra M, Brem EA, Nair S, Scheinberg P, Pereira J, Shune L, Joffe E, Young P, Spruill S, Katkov A, McRae R, Royston I, Faller DV, Rojkjaer L, Porcu P. 2023. Targeted therapy with nanatinostat and valganciclovir in recurrent EBV-positive lymphoid malignancies: a phase 1b/2 study. Blood Adv 7:6339–6350. https://doi.org/10.1182/bloodadvances.2023010330
45. Banerji U, van Doorn L, Papadatos-Pastos D, Kristeleit R, Debnam P, Tall M, Stewart A, Raynaud F, Garrett MD, Toal M, Hooftman L, De Bono JS, Verweij J, Eskens FA. 2012. A phase I pharmacokinetic and

pharmacodynamic study of CHR-3996, an oral class I selective histone deacetylase inhibitor in refractory solid tumors. Clin Cancer Res 18:2687–2694. https://doi.org/10.1158/1078-0432.CCR-11-3165
46. Marek M, Shaik TB, Heimburg T, Chakrabarti A, Lancelot J, Ramos-Morales E, Da Veiga C, Kalinin D, Melesina J, Robaa D, Schmidtkunz K, Suzuki T, Holl R, Ennifar E, Pierce RJ, Jung M, Sippl W, Romier C. 2018. Characterization of histone deacetylase 8 (HDAC8) selective inhibition reveals specific active site structural and functional determinants. J Med Chem 61:10000–10016. https://doi.org/10.1021/acs.jmedchem.8b01087
47. LaBonte MJ, Wilson PM, Fazzone W, Russell J, Louie SG, El-Khoueiry A, Lenz HJ, Ladner RD. 2011. The dual EGFR/HER2 inhibitor lapatinib synergistically enhances the antitumor activity of the histone deacetylase inhibitor panobinostat in colorectal cancer models. Cancer Res 71:3635–3648. https://doi.org/10.1158/0008-5472.CAN-10-2430